



**HAL**  
open science

## **Parametric study of propulsive forces in front crawl swimming: acceleration effect and flow behavior**

R Guignabel, Antoine Eon, Arnaud Decatoire, Tony Monnet, Laurent David,  
Mathias Samson

### ► **To cite this version:**

R Guignabel, Antoine Eon, Arnaud Decatoire, Tony Monnet, Laurent David, et al.. Parametric study of propulsive forces in front crawl swimming: acceleration effect and flow behavior. XIVth International Symposium of Biomechanics and Medicine in Swimming, Sep 2023, Leipzig, Germany. <hal-05033202>

**HAL Id: hal-05033202**

**<https://hal.science/hal-05033202v1>**

Submitted on 14 Apr 2025

**HAL** is a multi-disciplinary open access archive for the deposit and dissemination of scientific research documents, whether they are published or not. The documents may come from teaching and research institutions in France or abroad, or from public or private research centers.

L'archive ouverte pluridisciplinaire **HAL**, est destinée au dépôt et à la diffusion de documents scientifiques de niveau recherche, publiés ou non, émanant des établissements d'enseignement et de recherche français ou étrangers, des laboratoires publics ou privés.



Distributed under a Creative Commons CC BY 4.0 - Attribution - International License

# **PARAMETRIC STUDY OF PROPULSIVE FORCES IN FRONT CRAWL SWIMMING – ACCELERATION EFFECT AND FLOW BEHAVIOR**

R. Guignabel<sup>1</sup>, A. Eon<sup>1</sup>, A. Decatoire<sup>1</sup>, T. Monnet<sup>1</sup>, L. David<sup>1</sup> & M. Samson<sup>1</sup>, <sup>1</sup>Pprime Institute, CNRS – University of Poitiers – ENSMA, UPR 3346, Futuroscope Cedex, France

## **INTRODUCTION**

The arms play a key role in propulsion (Maglischo, 2003; Takagi et al., 2016). Numerous authors have studied the links between the kinematics of aquatic strokes of the upper limbs and propulsive forces, which are defined as the component of the resultant force in the swimming direction (Berger et al., 1999). The main kinematic parameters in optimising propulsive force have been shown by (Samson et al., 2015). Among these, arm acceleration holds an important place and many authors have studied its role in propulsion (Gardano & Dabnichki, 2006; Kudo et al., 2013; Rouboa et al., 2006; Sanders, 1999). Variations in velocities (accelerations) can generate up to 9 times more force than at constant velocity (Kudo et al., 2013). Although these studies have shown the relevance of acceleration in propulsion, to our knowledge, no parametric study has been carried out to model a relationship between acceleration and propulsive forces. To deepen our understanding of propulsive forces in relation to acceleration, we carried out a parametric experiment under unsteady conditions using a robotic device. The purpose of this paper is to study the role of acceleration on arm propulsion from a basic rotation movement. This work is based on both force and fluid velocity measures, from a robotic arm. Concurrently, a CFD study has been carried out. In so doing, we were able to experimentally observe the evolution of propulsive force versus acceleration (force measurements). Simultaneously, experimental and numerical 2D-PIV fields have enabled us to understand the phenomena (vortex dynamic and flow behaviour around swimmers' arms) behind the generation of these forces.

## METHODS

The robotic system described in Figure 1 is based on the swimmers' kinematics that we tend to reproduce by varying the angular acceleration of the arm  $\ddot{\theta}$  in  $\text{rad/s}^2$ . The aim is to produce a parametric study consisting of key parameters such as arm angular accelerations and propulsive forces, and then compare them with various phenomena such as vortex development and vortex detachment.

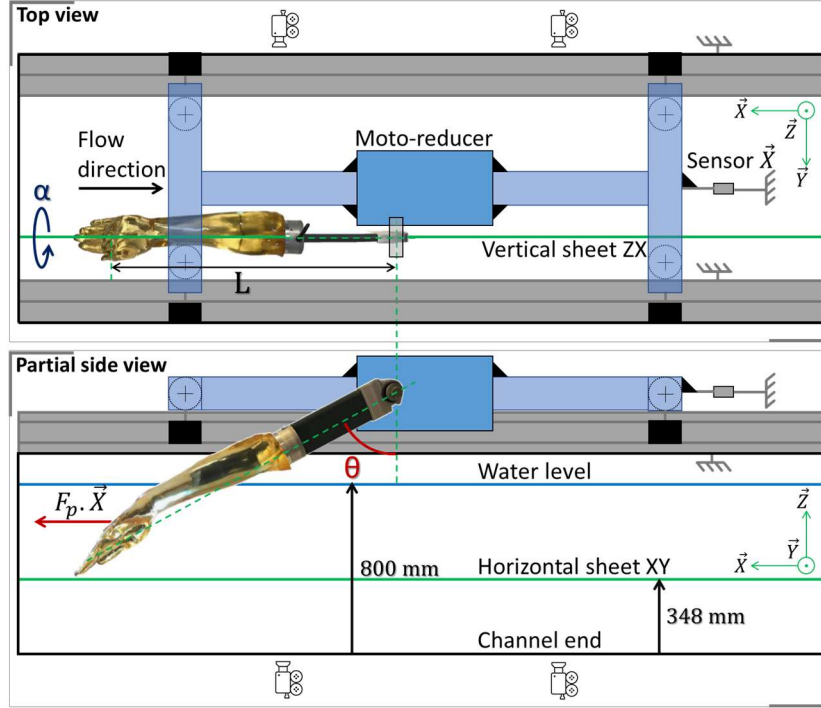


Figure 1: Schematic of the robotic arm device

We experimented in an open channel (relative flow rate of 0.3 m/s) (Figure 1). The system, comprising the molded arm of an elite swimmer (epoxy resin, density of 0.98 kg/L similar to the human body) and a moto-reducer, enabled the arm to be rotated from its shoulder axis, producing aquatic movements. The device produced arm strokes in water but was retained by a single-axis sensor, returning the force generated by the reaction of water on the arm, which represents the arm's propulsive force  $\vec{F}_p = F_p \cdot \vec{X}$  (Figure 1). The sensor used is a Laumas®, IP68 (acquisition frequency 256 Hz; Measurement range 0 to 2000 N; Sensitivity 2 mV/V; Combined error of measurement  $\pm 0.02\%$ ). We used a level to align the  $\vec{X}$  axis and calibrated the system with a device comprised of weights, belt and pulley, identifying frictional forces of 2.3 N. The motor was attached to a frame resting on two rails with four guide rollers providing a quasi-slip connection. We assume that the sensor fully measures the horizontal force ( $\vec{X}$ ) due to the careful alignment of the sensor and the low coefficient of friction. The sensor was connected to the motor's servo-drive from where data were extracted. Data were then processed with Matlab R2020b and computed to retrieve  $\theta$  and  $F_p \cdot \vec{X}$  thanks to the motor's encoder. The results were obtained in the cartesian frame of reference related to the earth  $R(\vec{X}, \vec{Y}, \vec{Z})$ . We have chosen a simple command law for a first approach focused on acceleration. The result is constant acceleration (or deceleration) over the entire angular range of motion, from 20 to 160 degrees. The propulsive force depicted in Figure 3 corresponds to the mean propulsive force measured at each step of the arm's trajectory (Guignabel et al., 2022). The arm's angular acceleration  $\ddot{\theta}$  varied between 1 to 15  $\text{rad/s}^2$  with a step of 1  $\text{rad/s}^2$ . The experiments were coupled with PIV measurements in two planes (Figure 1). In the vertical laser plane ZX, we

can follow and evaluate the behaviour of the fluid around the arm in the median plane. For the horizontal XY plane, vortex slices can be observed at different depths of the laser plane crossing the arm. Two Phantom v2640 cameras were used in single mode to be able to reconstruct the image for the whole motion  $\theta$  in degrees from  $20^\circ$  to  $160^\circ$ . There were 4 trials for each constant angular acceleration ranging from 1 to 10  $\text{rad/s}^2$  for each plane and 2 trials for angular accelerations ranging from 11 to 15  $\text{rad/s}^2$  in the vertical plane. The same tests were carried out with CFD using the URANS methodology (Samson et al., 2017).

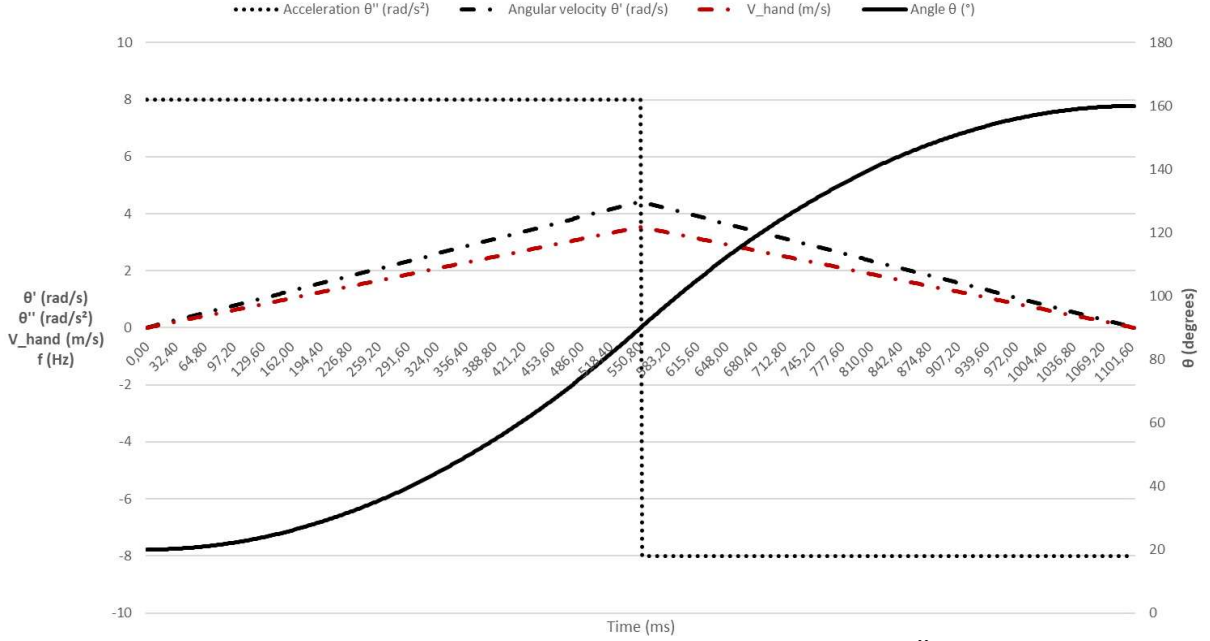


Figure 2: Example of the robotic device command law, for  $\ddot{\theta} = 8 \text{ rad/s}^2$

We wanted the acceleration to be constant on the arm's trajectory, so we could be able to assess the mean propulsive force on the overall path as well. Although we deviate from real swimming trajectories, it is preferred to focus on the effect of acceleration in propulsion in the context of a parametric study. However, accelerations of the arm were chosen so as to approach the actual conditions of swimming. We wanted a span of velocities of the hand between the paces of long-distance and sprint events. The arm's angular velocity  $\dot{\theta}$  varied from 1.6 to 6  $\text{rad/s}$  which implies the hand's velocity  $V_{hand}$  varying between 1.25 to 4.8  $\text{m/s}$  and the hand's acceleration  $\Gamma_{hand}$  between 2.2 to 31.2  $\text{m/s}^2$  in the cartesian frame of reference related to the earth  $R(\vec{X}, \vec{Y}, \vec{Z})$ :

*Equation 1 : Hand velocity*

$$\|\vec{V}_{hand}\| = L \times |\dot{\theta}| \quad (1)$$

*Equation 2 : Hand acceleration*

$$\|\vec{\Gamma}_{hand}\| = L\sqrt{\dot{\theta}^4 + \ddot{\theta}^2} \quad (2)$$

## RESULTS

### I. Force measurements

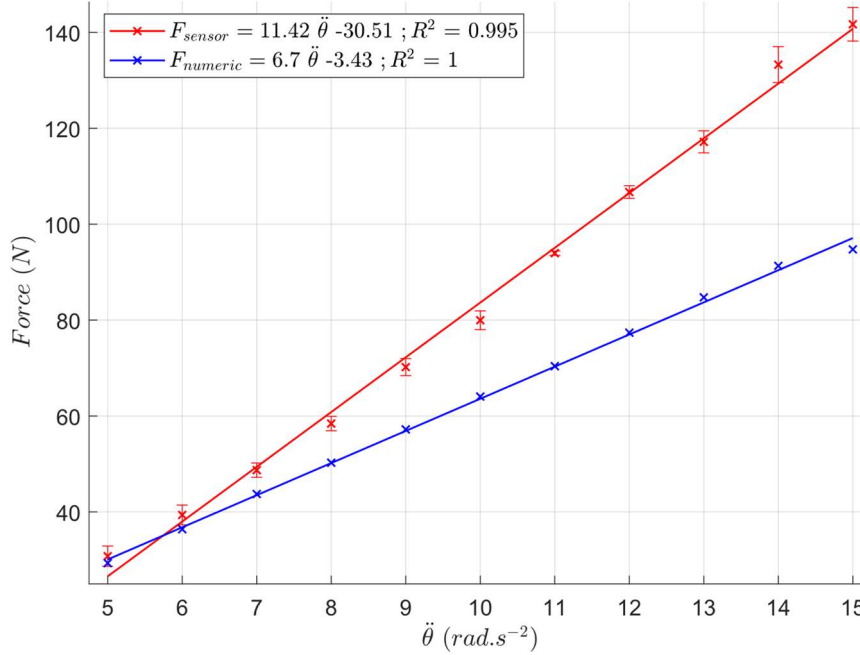


Figure 3: Mean propulsive force according to the arm angular acceleration.  $\times$  measured and calculated values, - interpolation.  $\bar{\sigma}$  standard deviation. Angular motion  $\theta$  from  $35^\circ$  to  $135^\circ$ .

The striking observation is the linear evolution of propulsive forces regarding the arm's acceleration. Force values range from 25 to 140 N, with different slopes between CFD and sensor measured values. The lower the accelerations, the closer the experimental and numerical values are. However, as acceleration values increase, the gap between our experimental measurements and numerical simulation widens. This is undoubtedly due to the URANS model used, which, although quite good at low accelerations, has its limitations in the presence of significant turbulence. One way of overcoming these discrepancies would be to turn to the Large Eddy Simulation (LES) model. This model filters the turbulence spectrum, large scales are computationally captured, small scales modelled as above. Thus, we could reduce deviations in the event of severe turbulence. However, this model requires enormous computing power.

## II. PIV measures & Computational Fluid Dynamics

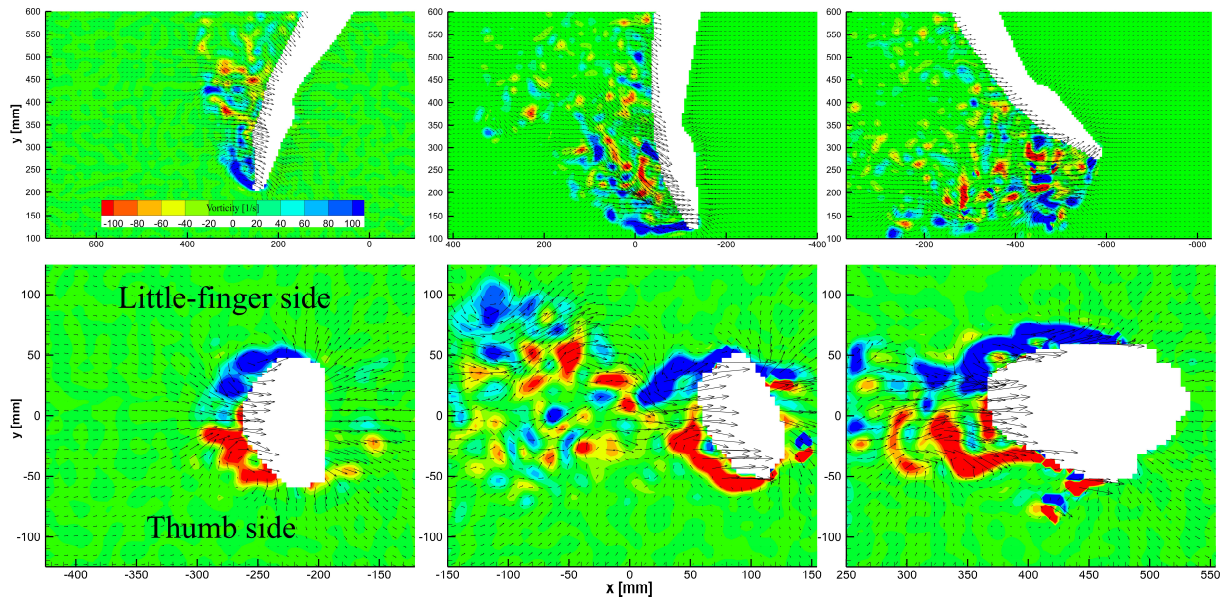


Figure 4: Experimental 2D-PIV fields for  $\ddot{\theta} = 8 \text{ rad/s}^2$ ;  $\theta = [60^\circ, 90^\circ, 120^\circ]$  for the ZX and XY laser planes.



Figure 5: Vorticity, obtained by CFD, for  $\ddot{\theta} = 8 \text{ rad/s}^2$ ;  $\theta = [60^\circ, 90^\circ, 120^\circ]$  at the same PIV laser planes.

For  $\theta = 60^\circ$ , we can see two vortex structures being formed on the edges of the thumb and little-finger (Figure 4). These vortices created under-pressure zones that strongly contributed to the generation of propulsive forces. Vortices grew and developed until the vertical position ( $\theta = 90^\circ$ ), and shedded in the wake due to the effects of the pressure gradient and the turbulent conditions. On vertical planes, we can observe a complex entanglement of vortex structures that appeared on the dorsal side of the hand, due to an accumulation of vorticity. These 2D-PIV visualisations showed a very three-dimensional flow with fluctuating vortices in all three

dimensions of space. There is also a tip vortex (TP) at the fingertips, caused by the pressure gradients between the palm and the dorsal side of the hand. The greater the acceleration of the arm, the greater the detachment and the more turbulent the wake. From  $\theta = 90^\circ$  to  $120^\circ$ , the wake became increasingly turbulent. To strengthen our understanding of the flow, we performed the same tests under numerical conditions (Figure 5), using the URANS methodology.

## DISCUSSION

Experimental and numerical measurements showed a linear evolution of propulsive force as a function of the arm angular acceleration with a satisfactory goodness of fit ( $R^2 = 0.99$ ). Our results showcase the importance of acceleration in the generation of propulsive forces. Indeed, it is easier for a swimmer to create high acceleration values on a short time rather than high velocity values. Acceleration values [Equation 1] can be in the range of 7 to 29  $m/s^2$  and quickly vary, while velocity values [Equation 2] can be in the range of 1.75 to 3  $m/s$  in average (Samson et al., 2015). Thus, swimmers would have to focus on velocity changes (accelerations), while generating high velocities. The underlying phenomena are difficult to study because the flow is turbulent and three-dimensional. In this study, only two vortices are clearly visible: one formed behind the hand and forearm and the other on the edges of the thumb and little finger. Upgrading the numerical model could enable us to better understand the mechanisms originating propulsive forces.

## ACKNOWLEDGEMENT

Authors would thank Patrick Braud, Jean-Carl Rousseau and Richard Tessier. Authors would also like to thank the Pprime Institute for the financial support provided (ACI project), and the French government aid managed by the National Research Agency (ANR) under the Future Investment Program (PIA) with the reference ANR-19-STHP-0001. This work pertains to the French government program “Investissements d’Avenir” (EUR INTREE, reference ANR-18-EURE-0010).

## REFERENCES

- Berger, M. A., Hollander, A. P., & de Groot, G. (1999). Determining propulsive force in front crawl swimming : A comparison of two methods. *Journal of Sports Sciences*, 17(2), 97-105.
- Gardano, P., & Dabnichki, P. (2006). Application of Boundary Element Method to modelling of added mass and its effect on hydrodynamic forces. *CMES - Computer Modeling in Engineering and Sciences*, 15, 87-98.
- Guignabel, R., Eon, A., Decatoire, A., Outada, A., & Samson, M. (2022). Parametric study of propulsive forces in front crawl swimming. *Computer Methods in Biomechanics and Biomedical Engineering*, 25(sup1), S134-S136.
- Kudo, S., Vennell, R., & Wilson, B. (2013). The effect of unsteady flow due to acceleration on hydrodynamic forces acting on the hand in swimming. *Journal of Biomechanics*, 46(10), 1697-1704.
- Maglischo, E. W. (2003). *Swimming fastest* (rev. edition). Human Kinetics.
- Rouboa, A., Silva, A., Leal, L., Rocha, J., & Alves, F. (2006). The effect of swimmer’s hand/forearm acceleration on propulsive forces generation using computational fluid dynamics. *Journal of Biomechanics*, 39(7), 1239-1248.
- Samson, M., Bernard, A., Monnet, T., Lacouture, P., & David, L. (2017). Unsteady computational fluid dynamics in front crawl swimming. *Computer Methods in Biomechanics and Biomedical Engineering*, 20(7), 783-793.
- Samson, M., Monnet, T., Bernard, A., Lacouture, P., & David, L. (2015). Kinematic hand parameters in front crawl at different paces of swimming. *Journal of Biomechanics*, 48(14), 3743-3750.
- Sanders, R. H. (1999). Hydrodynamic Characteristics of a Swimmer’s Hand. *Journal of Applied Biomechanics*, 15(1), 3-26.
- Takagi, H., Nakashima, M., Sato, Y., Matsuchi, K., & Sanders, R. H. (2016). Numerical and experimental investigations of human swimming motions. *Journal of Sports Sciences*, 34(16), 1564-1580.